International Journal of Research in Engineering and Science (IJRES)
ISSN (Online): 2320-9364, ISSN (Print): 2320-9356
www.ijres.org Volume 14 Issue 11 ǁ November 2026 ǁ PP. 87-98

Design of an Egg-Shaped Roly-Poly Bumper Car Based on Centre-of-Gravity Self-Balancing

XIAOXIAO ZHANG
(Shanghai University of Engineering Science, Shanghai, China,201620)

Abstract: *To overcome the problems of conventional bumper cars, namely fixed cockpits that cannot convey the mechanical process of a collision, passive rocking mechanisms with poor controllability, and a seat height that cannot accommodate occupants of different builds, a parent-child bumper car integrating the centre-of-gravity self-balancing principle of a roly-poly toy with omnidirectional mobility is designed. The vehicle consists of an egg-shaped cockpit, a crank-and-linkage controllable rocking mechanism, a gravity-adaptive lifting seat and a four-wheel Mecanum chassis: a low-centre-of-gravity counterweighted configuration provides a natural restoring moment; a servo motor drives a crank-and-rocker four-bar linkage to produce graded rocking according to the collision impact intensity; pressure sensors under the seat together with a screw-lifting mechanism adjust the seat height so as to constrain the centre of gravity of the whole vehicle in accordance with the occupant weight; and four independently driven Mecanum wheels achieve zero-radius spinning and lateral translation. The cockpit configuration was compared and selected, the tilt angle and the driving torque were verified, and the cross-sections of the links were sized and checked; a scaled prototype was then fabricated and functionally tested. The results show that under a collision at 2 m/s the egg-shaped cockpit reaches a maximum stress of about 0.29 MPa with a safety factor of about 69 and a fatigue life of more than one hundred million cycles, its comprehensive performance being superior to that of the square and spherical configurations; the overturning moment of the rocking mechanism at the 20-degree tilt limit is 51.3 N*m, the required torque calculated with a safety factor of 2 is 102.6 N*m, and the selected servo gear motor delivers 112.2 N*m, meeting the requirement; with a 16 mm connecting rod the buckling safety factor is 2.42 and the bending stress is 103.3 MPa, both within the allowable values. The prototype reproduces collision-graded rocking, weight-limited seat lifting and omnidirectional movement, confirming the feasibility of the scheme.*

Keywords: *bumper car; roly-poly; centre-of-gravity self-balancing; crank-and-linkage mechanism; Mecanum wheel; amusement ride safety*

Date of Submission: 28-10-2026 Date of acceptance: 07-11-2026

I. Introduction

With the continuous advancement of urbanization and profound changes in family parenting concepts, the design paradigm of contemporary urban public spaces and playground environments is shifting from a single entertainment function to a composite one that integrates humanistic care, ecological integration and science education. As an important vehicle for children's outdoor leisure and for the development of their physical and mental abilities, parent-child amusement facilities must not only satisfy the basic right to play and the relevant safety regulations, but also carry the deeper social expectation of promoting interaction between generations and inspiring scientific cognition. The concept of "learning through play" has gradually become the core idea in playground design, that is, embedding scientific principles into the play experience so that children complete their cognition and exploration of the objective world while playing.

However, traditional mechanical amusement facilities such as bumper cars (Fig. 1a), although able to provide intense collision stimulation and emotional release, confine the experience to planar displacement and impact because of their fixed cockpit, lacking a deep bodily perception of the dynamic mechanical changes during a collision and thus failing to convey physical concepts such as the centre of gravity, balance and restoring moment in an intuitive way. At the same time, a fixed seat height cannot accommodate occupants of different builds and weights, and a heavy occupant tends to raise the centre of gravity of the whole vehicle. In addition, existing rocking devices rely mostly on springs to achieve passive rocking, in which the swing amplitude fluctuates sharply with the impact force, the restoring moment is nonlinear, and the fatigue life of the spring is short, making it difficult to guarantee both the consistency of the experience and safety.

As a traditional Chinese toy, the roly-poly, by virtue of its mechanical configuration of "light on top and heavy at the bottom; the lower the centre of gravity, the more stable", possesses excellent resistance to external disturbance and the ability to restore equilibrium. If this centre-of-gravity self-balancing model is introduced

into the cockpit of a bumper car, abstract mechanical principles can be transformed into an immersive bodily experience (Fig. 1b).



Fig. 1 A conventional bumper car and the concept proposed in this paper
(a) conventional bumper car; (b) concept of the egg-shaped roly-poly bumper car

With regard to engineering practice, considerable research has been conducted on the collision dynamics and occupant kinematics of bumper cars: Zhao carried out a simulation of the low-speed collision process of bumper cars based on transient dynamics [2] and analysed the collision response and safety at different impact speeds [11]; Cohen et al. investigated, through full-scale tests, the vehicle and occupant kinematics of bumper cars under frontal, lateral and free-operation impacts [6]; and Smith et al. analysed the crashworthiness of foam-filled bumper beams under low-speed impact [9]. At the level of standards, GB 8408-2018 "Safety specification for large-scale amusement devices" [1], ASTM F2291-16 [7] and ISO 17842-1:2023 [8] impose mandatory requirements on the mechanism design, tilt limits and emergency braking devices of amusement rides respectively. Existing studies mostly focus on collision safety and structural strength, whereas an overall vehicle scheme that takes the closed-loop bodily sensation of "collision—swing—recovery" as its design objective and at the same time accommodates centre-of-gravity adaptation for occupants of different builds is rarely seen.

Therefore, this paper designs an egg-shaped roly-poly bumper car. The main work comprises: (1) replacing the traditional fixed cabin with a bionic egg-shaped cockpit and determining, through configuration comparison, the cabin form that gives the best compromise among strength, space utilization and ergonomics; (2) replacing passive spring recovery with a crank-and-rocker four-bar linkage driven by a servo motor, so as to achieve controllable rocking that is graded according to the collision intensity and can be actively returned to the neutral position; (3) constructing an adaptive seat from gravity sensors and a screw-lifting mechanism, which limits the adjustment range of the centre of gravity according to the occupant weight; and (4) replacing the two-wheel differential chassis with four Mecanum wheels, so as to realize omnidirectional movement with a zero turning radius. On this basis, the mechanical verification of the whole vehicle and the fabrication of a prototype were completed, and the feasibility of the scheme was verified through functional tests.

II. Overall Design

2.1 Design Objectives and Overall Configuration

The objective of this design is to transform the collision process into a perceptible, controllable and repeatable rocking sensation while satisfying the requirements of GB 8408-2018, and to take into account parent-child interaction and the popularization of the centre-of-gravity principle. The vehicle adopts a three-layer configuration of "upper egg-shaped cockpit—middle controllable rocking mechanism—lower counterweighted chassis", as shown in Fig. 2.

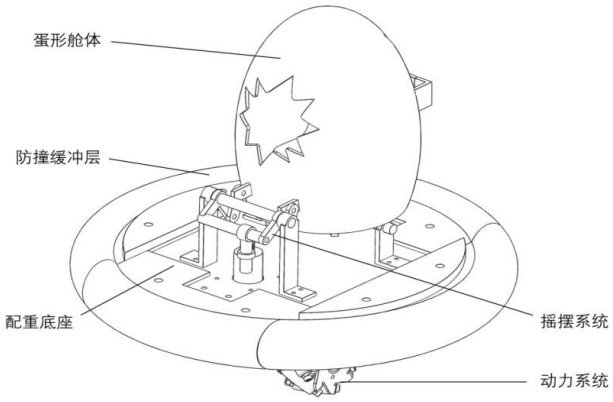


Fig. 2 Overall mechanism of the egg-shaped roly-poly bumper car

The upper layer is a fully enclosed egg-shaped cockpit that provides an immersive riding space; the middle layer is the crank-and-linkage rocking mechanism, which is installed between the cockpit and the chassis and is the core motion unit; the lower layer is the counterweighted chassis, in which cast-iron counterweight blocks are built into a closed cavity so that the centre of gravity of the whole vehicle is stably kept below one third of its height. An EVA anti-collision buffer layer 50 mm thick is provided between the cockpit and the base, and polyurethane anti-collision strips of not less than 50 mm are additionally fitted around the vehicle body. The whole vehicle adopts a strictly "light on top, heavy at the bottom" mass distribution: whichever side the cockpit tilts towards, the line of action of the gravity of the whole vehicle always produces a restoring moment about the tilting fulcrum, which is both the source of the roly-poly self-balancing characteristic and the mechanical safety fallback in the event of electrical control failure.

2.2 User Demand Survey

To determine the functional priorities and the ergonomic parameters, a questionnaire was distributed among parent-child families, covering eight dimensions: the most interesting feature, the soft-collision experience, acceptance of the safety configuration, interest in extended game modes, educational value, parent-child interaction, willingness to try, and preference between vehicle types. Four representative results are shown in Fig. 3.

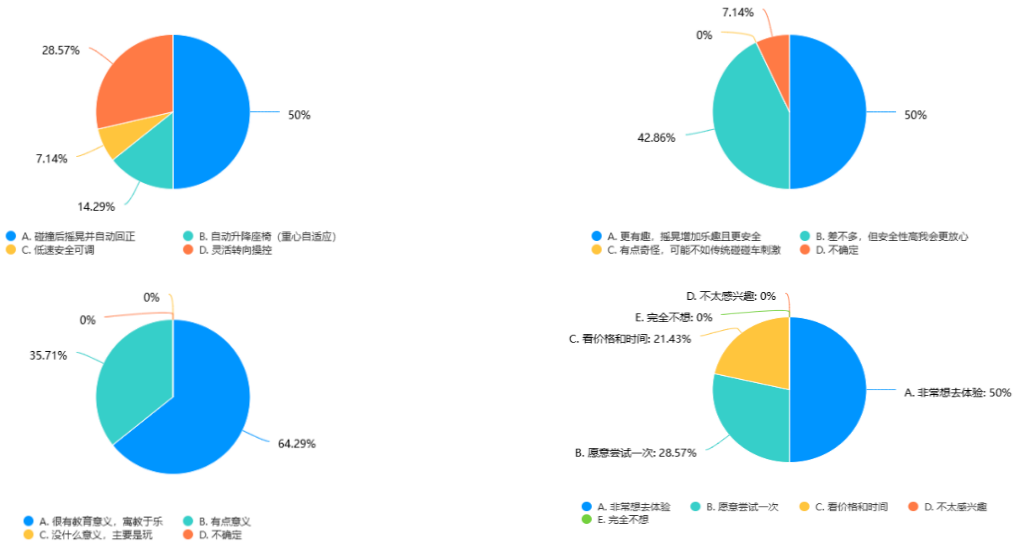


Fig. 3 Results of the user demand survey
(a) most interesting feature; (b) amusement value of the soft-collision experience; (c) educational value of physical knowledge; (d) willingness to try

The survey shows that 50.00% of the respondents ranked "rocking after a collision and automatic recovery" as the most interesting feature, followed by "agile steering and handling" (28.57%); more than half of the respondents considered the soft-collision experience of "slight rocking and then recovery after a collision" to

be more interesting and safer than the hard collision of a conventional bumper car; nearly 80% approved the safety protection configuration of the product; more than 90% were interested in rule-based competitive game modes; most respondents believed that the product could help children understand physical knowledge such as the centre of gravity, balance and recovery, and could significantly enhance parent-child interaction; and when the product was placed in a shopping mall children's area or an amusement park, more than 70% of the respondents expressed a willingness to try it with no obvious resistance. The survey results determined the functional architecture with controllable rocking as the core, omnidirectional mobility and the adaptive seat as the support, and competitive game modes as the extension.

2.3 Pain Point Analysis and Countermeasures

With regard to the four pain points of conventional bumper cars in handling, collision sensation, occupant adaptability, and safety versus economy, this design proposes corresponding technical countermeasures item by item, as shown in Table 1.

Table 1 Main pain points of conventional bumper cars and the countermeasures proposed in this paper

Pain point	Specific manifestation	Technical countermeasure in this paper
Limited handling	The minimum turning radius of the two-wheel differential chassis is 0.5 m, making steering and avoidance in narrow sites cumbersome	Four independently driven Mecanum wheels; zero turning radius; lateral translation and on-the-spot spinning are supported
Single collision sensation	The fixed cockpit can only achieve planar impact, with no perception of the mechanical process of a collision	An egg-shaped cockpit combined with crank-and-linkage rocking; graded rocking and automatic recovery after a collision
Poor occupant adaptability	The seat height is fixed; a heavy occupant raises the centre of gravity of the whole vehicle and causes excessive swing	Gravity sensors combined with a screw-lifting seat; the adjustment range of the centre of gravity is limited according to body weight
Conflict between safety and economy	High investment in conductive floors and overhead grids, with a hidden danger of electric leakage; springs are prone to fatigue	The conductive-floor scheme is eliminated; dual electrical-control and gravity recovery, with triple redundant protection

2.4 Main Technical Parameters

Based on the ergonomic data, the results of power matching and the requirements of the safety codes, the main technical parameters of the whole vehicle are determined as shown in Table 2.

Table 2 Main technical parameters of the whole vehicle

Item	Value
Number of occupants per ride	1–2
Overall dimensions (L × W × H)	1500 mm × 1500 mm × 1750 mm
Total mass	about 153 kg (including the counterweight base, battery and motors)
Recommended site size	15 m × 15 m
Drive mode	24 V DC gear motors × 4; four Mecanum wheels driven independently
Operating speed	0–1.5 m/s, with a default speed limit of 1.2 m/s
Maximum acceleration	≤0.5 m/s^2
Maximum cockpit tilt angle	20° (constrained by both the electronic soft limit and the mechanical hard limit)
Seat centre-of-gravity adjustment range	10–20 cm for a body weight below 60 kg; 5–10 cm for 60 kg and above
Battery and endurance	24 V 32 Ah lead-acid battery; endurance ≥ 4 h
Main control unit	Siemens S7-200 SMART PLC; response delay ≤ 100 ms

III. Design of the Key Mechanisms

3.1 Egg-Shaped Cockpit Configuration and Strength Analysis

The cockpit configuration must simultaneously satisfy four requirements: collision safety, space utilization, ergonomics and manufacturing cost. Taking a total mass of 135 kg, a maximum collision speed of 2 m/s, a contact time of 0.1 s (average impact force 2700 N) and a wall thickness of 10 mm as the basic operating conditions, three typical configurations of a glass-fibre-reinforced plastic (FRP; density 1.7 g/cm^3, elastic modulus 16.7 GPa, tensile strength 300 MPa, fatigue strength about 20 MPa) cockpit are compared, and the results are shown in Table 3.

Table 3 Comparison of the mechanical performance of three cockpit configurations

Configuration	Maximum stress / MPa	Safety factor	Fatigue life	Space utilization	Comprehensive evaluation
Square	1.6–2.4	≈ 8.3	about 50 million cycles	baseline	The stress concentration factor at the right angle is about 3.0; flat plates are prone to local denting and stiffeners are required
Spherical	≈ 0.09	≈ 222	—	about 60% of the square one	The best mechanical performance, but getting in and out is inconvenient, seat installation is complex and the cost is high
Egg-shaped	≈ 0.29	≈ 69	more than 100 million cycles	more than 30% higher than the spherical one	No stress concentration point; energy is absorbed by progressive buckling; the best overall compromise

For the square cockpit, because the stress concentration factor at the right angle is about 3.0, the dynamic maximum stress reaches 1.6–2.4 MPa, the safety factor is about 8.3 and the fatigue life is about 50 million cycles; its flat-plate structure is prone to local denting and requires additional stiffeners, which instead increases the weight and the cost. The spherical cockpit has the best mechanical performance, with a maximum stress of about 0.09 MPa and a safety factor of about 222, but its space utilization is only 60% of that of the square one, making it inconvenient to get in and out, complex to install the seat, and expensive to manufacture. The egg-shaped cockpit has a maximum stress of about 0.29 MPa, a safety factor of about 69 and a fatigue life of more than 100 million cycles; it has no stress concentration point, can absorb impact energy uniformly through progressive buckling and avoid brittle fracture, and its space utilization is more than 30% higher than that of the spherical one.

From the point of view of the load-bearing mechanism, the positive Gaussian curvature of the egg-shaped shell spreads the impact load uniformly along the curved surface, avoiding the stress concentration at the edges and corners of a square shell; the rounded outline without edges and corners reduces the local pressure during a collision and is also in harmony with the dinosaur-egg IP image. Considering mechanical performance, space utilization, ergonomics and manufacturing cost comprehensively, the egg-shaped configuration is the optimal compromise under the above constraints and was therefore determined as the cockpit form.

3.2 Crank-and-Linkage Controllable Rocking Mechanism

The rocking actuator must simultaneously satisfy three requirements: the swing amplitude can be graded according to the collision intensity, the recovery is smooth without jolting, and no failure occurs under long-term high-frequency reciprocation. To this end, three schemes are compared, as shown in Table 4.

Table 4 Comparison of three rocking drive schemes

Scheme	Drive mode	Controllability of the swing	Recovery mode	Key defect	Conclusion
Pure spring	none	uncontrollable, fluctuating sharply with the impact force	elastic recovery by the spring	nonlinear restoring moment and easy jolting; fatigue life of about 500 000 cycles; the whole set must be replaced after ageing	rejected
Pure ball joint, no drive	none	completely uncontrollable	no recovery element	remains tilted after a collision; risk of overturning; does not meet the mandatory anti-overturning requirement	rejected
Servo motor with crank and linkage	servo gear motor	controllable in three levels according to the impact intensity	active motor recovery + passive gravity recovery by the counterweight	the mechanism is relatively complex and the control parameters need to be coordinated	selected

The pure-spring recovery scheme relies on symmetrically arranged compression springs around the cockpit to provide the restoring moment; it has no active drive unit and only rocks passively under the collision impact. Its swing amplitude is uncontrollable and the swing angle varies greatly with different collision forces; the restoring moment is nonlinear, the recovery being slow under a small impact and the spring rebound being violent under a large impact, which easily causes jolting of the occupants; it has no graded interaction capability; the fatigue life of the spring is only about 500 000 cycles, and the attenuation of its stiffness in the later period leads to swing deviation and abnormal noise, with the result that the whole set of elastic elements must be replaced after batch ageing. The pure-ball-joint, no-drive scheme relies only on a ball universal joint to achieve free deflection of the cockpit; it has neither a drive nor a recovery element, so the cockpit remains tilted after a collision and cannot return to its original position by itself, which presents an overturning risk and does not meet the mandatory anti-overturning requirement for amusement facilities.

The motor-driven crank-and-linkage scheme uses a 24 V servo gear motor as the power source. The motor output shaft is connected to an eccentric crank disc, and the crank is connected to the rocker arm at the

bottom of the cockpit through an articulated connecting rod; as the motor rotates at a uniform speed, the crank performs circular motion, and the connecting rod converts the circular motion into reciprocating swing of the rocker arm, which in turn drives the cockpit to produce a controllable tilt; when the motor stops driving, the constant gravitational restoring moment provided by the bottom counterweight automatically pulls the cockpit back to the neutral position (Fig. 4). This scheme constitutes a dual system of "electronically controlled active swing + gravity-driven passive recovery": it retains the low-centre-of-gravity self-balancing characteristic of the roly-poly while acquiring the ability to control the swing amplitude and duration by programming, so that three levels of swing commands, namely light, medium and heavy, can be issued according to the collision intensity. Considering controllability, service life and safety redundancy comprehensively, this scheme was selected as the rocking actuator.

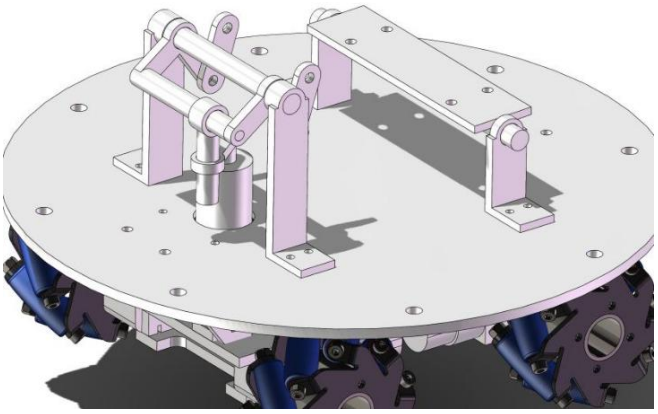


Fig. 4 Crank-and-linkage rocking mechanism

The response process of the cockpit after a collision is shown in Fig. 5: the collision impact is transmitted through the cabin to the chassis, the main controller outputs a swing command according to the impact intensity, the cockpit tilts in the impact direction about the swing fulcrum, and is then restored by the joint action of the active motor recovery and the counterweight gravity, forming a complete bodily-sensation loop of "collision—tilt—recovery".

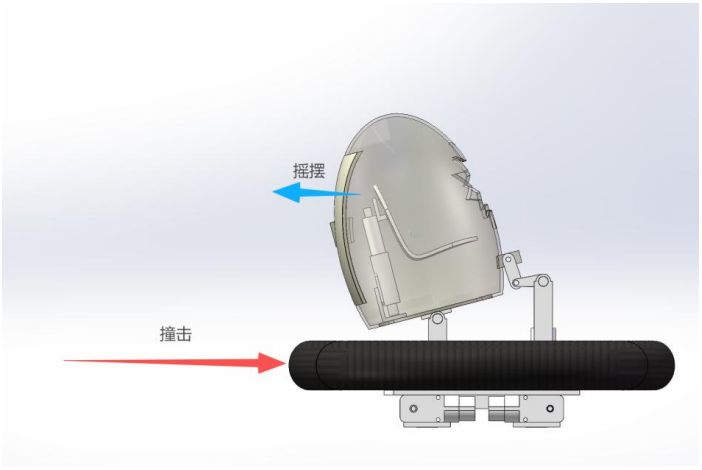


Fig. 5 Collision—rocking response of the cockpit

The tilt angle and the driving torque are verified as follows. The total mass of the whole vehicle is M = 153 kg and the total gravity is G = Mg = 1499.4 N; the design maximum tilt angle is $\theta_{max} = 20°$; the horizontal eccentricity between the swing centre and the centre of gravity of the whole vehicle is e = 0.1 m. When the cockpit tilts to the limit condition, the overturning moment produced by gravity about the swing centre is

$$M_{over} = G \cdot e \cdot \sin\theta_{max} = 1499.4 \times 0.1 \times \sin 20° \approx 51.3 \text{ N·m}$$

With a safety factor of n = 2, the minimum output torque required of the rocking mechanism is

$$T_{need} = n \cdot M_{over} = 2 \times 51.3 = 102.6 \text{ N·m}$$

A 24 V servo gear motor is selected, with a rated torque $T_m = 2.2$ N·m, a reduction ratio i = 60 and a mechanical transmission efficiency $\eta = 0.85$. The theoretical output torque after reduction is

$$T_{out} = T_m \cdot i \cdot \eta = 2.2 \times 60 \times 0.85 = 112.2 \text{ N·m} > 102.6 \text{ N·m}$$

The calculation shows that the motor output torque meets the requirement with a margin of about 9.4%, so 112.2 N·m is taken as the basis for the force calculation of the four-bar mechanism.

The four-bar mechanism consists of the crank r, the frame a, the connecting rod L and the rocker arm R. Limited by the 220 mm vertical installation gap between the cockpit and the base, the upper limit of the rocker arm length is taken as 220 mm: if it is larger than 220 mm, the connecting rod will interfere with the counterweight base during swinging; if it is smaller than 220 mm, the maximum tilt angle of the cockpit will be less than 20° for the same crank stroke, so that the swinging sensation will be too weak. The crank eccentricity directly determines the swing stroke of the rocker arm; it is verified by three-dimensional geometric simulation that with r = 20 mm the maximum swing angle of the rocker arm is exactly 20°. The frame length is constrained by the installation position in the motor compartment and is taken as a = 160 mm, and the connecting rod is taken as L = 180 mm. The Grashof criterion for a crank undergoing complete rotation is then checked:

$$r + R = 20 + 220 = 240 \text{ mm} < a + L = 160 + 180 = 340 \text{ mm}$$

The criterion is satisfied, the mechanism has no dead point, and the crank can rotate continuously through 360°.

All four bars are made of quenched and tempered 45 steel, with a yield strength σ_s = 355 MPa, an allowable bending stress [σ] = 120 MPa (the dynamic-load safety factor is taken as 3) and an elastic modulus E = 206 GPa. The maximum axial compressive force in the connecting rod under the limit condition is determined from the moment balance:

$$F_{rod} = T_{out}/r = 112.2/0.02 = 5\,610 \text{ N}$$

With the additional collision impact load of 2700 N superimposed, the composite peak load in the connecting rod is F_{max} = 8310 N. The connecting rod is selected as a solid round bar of 16 mm in diameter; the second moment of area of the cross-section is $I = \pi d^4/64 \approx 3.217 \times 10^{-9}$ m^4, and the buckling critical force is calculated by the Euler formula:

$$F_{cr} = \pi^2 EI/L^2 \approx 20\,140 \text{ N}$$

The buckling safety factor is $n_{stab} = 20\,140/8310 \approx 2.42 > 2$, which meets the dynamic-load stability requirement for amusement devices. With an eccentric load arm of 5 mm for a lateral collision, the maximum bending moment is M_{rod} = 41.55 N·m, the section modulus in bending is $W_z = \pi d^3/32 \approx 4.021 \times 10^{-7}$ m^3, and the bending stress is σ = 103.3 MPa < [σ] = 120 MPa, meeting the strength requirement. If the rod diameter is reduced to 12 mm, the buckling safety factor is only 1.12; if it is increased to 20 mm, the self-weight of the bar increases by 36% and the inertia of the mechanism becomes larger, making the rocking response sluggish. Therefore 16 mm is the reasonable value.

The rocker arm is made of a rectangular steel section of 40 mm × 10 mm, with a section modulus in bending of $W = bt^2/6 \approx 6.667 \times 10^{-7}$ m^3 and a bending stress of $\sigma = 51.3/(6.667 \times 10^{-7}) \approx 76.95$ MPa < 120 MPa; for the crank shaft, the minimum required diameter calculated from the torsional strength is $d \geq [16T_{out}/(\pi[\tau])]^{1/3} \approx 21$ mm ([τ] = 60 MPa). All the bars retain a sufficient strength margin.

3.3 Gravity-Adaptive Lifting Seat

In a conventional bumper car the seat height is fixed and cannot accommodate occupants of different builds: a heavy occupant raises the centre of gravity of the whole vehicle, causing an excessive swing amplitude during rocking. For this reason a gravity-adaptive lifting seat is designed (Fig. 6), consisting of three parts: sensing and detection, control, and mechanical transmission.

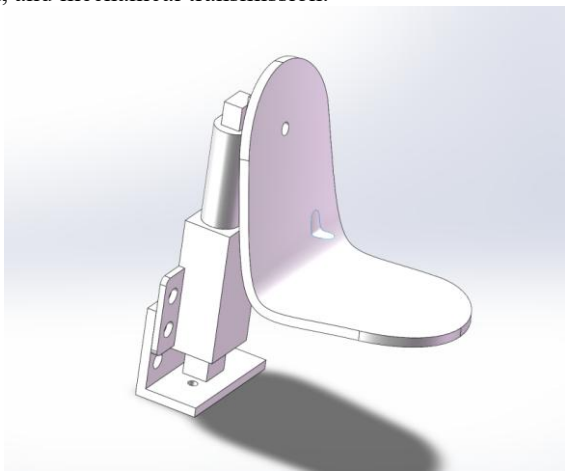


Fig. 6 Gravity-adaptive lifting seat

One gravity pressure sensor is arranged at each of the four corners of the seat base and, together with an A/D conversion module, detects the occupant weight and the forward—backward and left—right excursion of the centre of gravity; a displacement sensor additionally provides real-time feedback of the seat lifting height. The control core is a Siemens S7-200 SMART PLC, which performs data filtering, weight classification, height comparison and the control of the adjustment authority, with a system response delay of no more than 100 ms. The mechanical transmission is powered by a 24 V DC gear motor, and converts the rotary motion into the vertical lifting of the seat through a worm-and-worm-wheel reduction box and a trapezoidal screw; an optical shaft and a linear bearing are used for guidance to ensure smooth lifting, and limit switches are installed at the upper and lower ends as mechanical hard limits.

For safety, triple protection is adopted, comprising an electronic soft limit, a mechanical hard limit and self-locking of the mechanism: the adjustment range is divided into two levels according to body weight, the adjustable range of the seat centre of gravity being 10–20 cm for an occupant weighing less than 60 kg and being limited to 5–10 cm for an occupant weighing 60 kg or more; the system continuously compares the current seat height with the safety limit and immediately cuts off the power supply to the lifting motor when the upper limit is exceeded, and a forced shutdown is triggered when a limit switch is activated; the self-locking characteristic of the worm-and-worm-wheel pair and the trapezoidal screw ensures that the seat will not slide down by itself at any height. The device also has a science popularization function: the occupant can adjust the seat height personally and directly feel the change that "the lower the seat, the more stable; the higher the seat, the easier it is to shake", thereby transforming the abstract concept of "the lower the centre of gravity, the more stable" into a perceptible bodily experience.

3.4 Mecanum-Wheel Omnidirectional Chassis

The chassis is the load-bearing foundation of the whole vehicle and the execution core of the omnidirectional motion; it adopts an integrated welded frame of Q355B steel plate and integrates three modules: Mecanum wheel drive, peripheral anti-collision protection and adjustable counterweight (Fig. 7). The travelling system abandons the conventional two-wheel differential mechanism and adopts a scheme with four Mecanum wheels arranged independently at the four corners; each of the four wheels is equipped with a 24 V DC gear motor, and the four motors are independently closed-loop speed-controlled by the PLC, so that omnidirectional motion is achieved through the combination of the rotational speeds of the different wheels: the four wheels rotating in the same direction at the same speed produce straight forward or backward motion, the wheels on the left and right sides running in opposite directions at different speeds produce lateral translation, and the diagonal wheels rotating in opposite directions produce on-the-spot spinning with a zero radius.

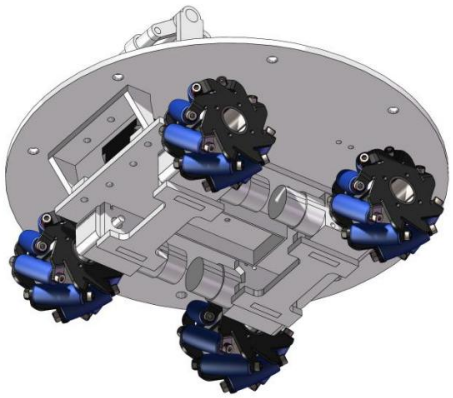


Fig. 7 Four-wheel Mecanum chassis

A 12-inch (300 mm) polyurethane fully covered Mecanum wheel is selected, with a thickened cast-aluminium hub and rollers covered with highly wear-resistant PU, and a wheel width of 50 mm. Compared with differential wheels, its advantages are: a higher degree of freedom of motion, supporting lateral translation, oblique sliding and on-the-spot spinning in addition to straight travel, with no need to reserve turning space; greater amusement value in handling, being suitable for competitive actions such as dodging and circling; and more uniform load distribution with four independently loaded wheels, so that the impact load on a single wheel is smaller.

The load-carrying capacity of the wheel is verified as follows. The rated load for a single occupant is taken as 90 kg; referring to the reasonable ratio interval of 0.6–0.8 between the kerb mass and the rated load for similar small passenger amusement vehicles, the value 0.7 is taken, giving an estimated kerb mass of 63 kg and a total design mass of the whole vehicle of 153 kg. With the four-wheel arrangement, the average static load per wheel is 153/4 = 38.25 kg. Considering the frequent starting and stopping, collisions and bumping, the safety factor is taken as 2 and the design load per wheel is 76.5 kg, so a wheel type with a rated load capacity of not less than 100 kg is selected.

The ground contact pressure is calculated as $P = F/(B \cdot L_e)$. The normal force corresponding to the design load per wheel is $F \approx 750$ N and the wheel width is $B = 50$ mm; since a Mecanum wheel contacts the ground through several groups of rollers, the equivalent contact length is taken as 18% of the wheel diameter, i.e. $L_e \approx 54$ mm, giving

$$P = 750/(50 \times 54) \approx 0.28 \text{ MPa}$$

This value is far below the allowable pressure interval of 0.5–0.8 MPa for the PU roller surface, so the pressure margin of the wheel surface is sufficient, and the structural reliability can be guaranteed under high-frequency collision and eccentric load conditions. Cast-iron counterweight blocks are built into the closed cavity of the chassis, so that the centre of gravity is kept below one third of the height of the whole vehicle; the arrangement of four wheels at the four corners enlarges the support base and, together with the angle limitation of the rocking mechanism, jointly avoids the risk of rollover.

IV. Control System and Safety Protection Design

4.1 System Composition and Working Principle

The control system of the whole vehicle is divided into five units: seat centre-of-gravity detection, crank-and-linkage rocking execution, Mecanum-wheel omnidirectional travelling drive, main-control PLC and safety monitoring. The seat sensing module consists of four gravity pressure sensors, an A/D module and a displacement sensor, and collects the occupant weight, the excursion of the centre of gravity and the seat height; distributed pressure sensors around the vehicle body collect the collision impact intensity and output the rocking control signal in a graded manner; a three-axis gyroscope built into the cockpit continuously collects the tilt angle and the angular velocity, forming the closed-loop control of the rocking mechanism; and each of the four hub motors is equipped with a Hall encoder to feed back the rotational speed and the stall state. The main control is a Siemens S7-200 SMART PLC, which uniformly performs multi-channel data filtering, weight classification, tilt angle limitation, omnidirectional motion solving, fault alarming and emergency-stop interlocking, with an overall response delay of no more than 100 ms.

The working process is as follows. After the occupant is seated, the gravity sensors transmit the weight and the centre-of-gravity data to the PLC, and the system matches the corresponding safe adjustment range of the seat according to the preset rules; when the occupant adjusts the seat, the displacement sensor feeds back the height in real time, and the lifting function is automatically locked when the upper limit corresponding to the body weight is reached. After the collision sensors detect an impact, the PLC divides the rocking command into three levels according to the impact intensity and controls the servo motor to drive the eccentric crank to rotate, so that the cockpit tilts reciprocally through the linkage transmission: a small-amplitude low-frequency swing for a light collision, a medium-amplitude reciprocating swing for a medium collision, and a full-amplitude short-duration swing for a heavy collision. The gyroscope monitors the tilt angle in real time, and once it exceeds the 20° design threshold, the power to the rocking motor is immediately cut off and an alarm is issued. After a single swing cycle ends, the PLC controls the motor to reverse so that the crank returns to the neutral position, completing the active recovery; in the case of a power failure or an emergency stop, the electromagnetic brake of the servo motor locks the crank, while the bottom counterweight produces a restoring moment under gravity, forming a double fallback. During travelling, the PLC has a built-in Mecanum-wheel motion solving algorithm, which decomposes the single-channel control signal from the handle into independent rotational-speed commands for the four motors, and the encoders correct the speed difference in closed loop to ensure smooth motion without drift.

4.2 Safety Protection Design

A safety system covering the mechanical mechanism, occupant restraint and electrical control is constructed around two directions: active prevention and passive fallback. With regard to the mechanical mechanism, the active defence relies on the closed-loop adjustment of the gravity sensors and the adaptive seat, together with the real-time monitoring of the cockpit attitude by the gyroscope, to lock the centre of gravity of the whole vehicle dynamically below the swing centre and to keep the maximum tilt angle within 20°; a dual mechanism of mechanical hard limit and electronic soft limit is used to cut off the power to the rocking motor and to issue an alarm when the limit is exceeded. The recovery function is provided with triple redundancy, namely the active recovery by the servo motor, the passive gravity recovery by the counterweight and the

restraint by the polyurethane buffer limit stops, so that the remaining mechanisms can still maintain a stable attitude of the cockpit after a single link fails. For passive defence, the chassis is integrally welded from Q235B steel plate and 100% of the key welds are subjected to non-destructive testing; polyurethane anti-collision strips of not less than 50 mm are fitted around the vehicle body, and protective strips are wrapped around sharp parts such as the windows; the cockpit is provided with an FRP buffer layer, and the door frame is made of high-strength alloy steel to avoid deformation of the cabin and to facilitate later rescue. In addition, a ratchet-and-pawl wheel-side locking mechanism is integrated on the inner side of each of the two driving wheels as the final mechanical line of defence in the event of loss of control of the vehicle, which meets the mandatory requirement for an emergency braking device in Clause 6.3.2 of GB 8408-2018.

With regard to occupant restraint, a combination of a two-point seat belt and a shoulder belt with a breaking tension of not less than 15 kN is adopted, which can be adjusted by the occupant to suit a height of 150–170 cm; a quick emergency hatch is provided on the side of the cockpit that can be unlocked manually in the event of a power failure; and the cockpit is equipped with anti-slip handrails of not less than 30 mm and guard rails of not less than 600 mm (Fig. 8).



Fig. 8 Occupant restraint and cockpit protection

With regard to electrical control, protection against overload, short circuit and electric leakage is provided (the leakage operating current being not more than 30 mA), the insulation resistance is not less than 1 MΩ, the earthing resistance is not more than 4 Ω, and the degree of protection is IP54; a closed-loop speed-regulating circuit composed of the servo drive and the speed encoder constrains the maximum linear velocity of the cockpit envelope to below 2 m/s, and a two-level interlock of the electronic overspeed criterion and the mechanical centrifugal speed limiter is provided; red emergency-stop buttons are installed in both the cockpit and the console, and a UPS emergency power supply is provided, which can maintain the operation of the system for not less than 30 min after a power failure, thus guaranteeing support for emergency handling and passenger evacuation.

V. Prototype Fabrication and Functional Verification

5.1 Prototype Fabrication

Based on the parameters and verification results described above, a scaled prototype was fabricated and assembled in proportion to the structure of the finished product (Fig. 9). The parts of the prototype are processed by combining 3D printing with wire-cut sheet metal: the complex irregular parts such as the egg-shaped cockpit shell, the crank, the connecting rod, the rocker arm and the seat bracket are integrally formed by 3D printing, whereas the straight load-bearing sheet metal parts such as the chassis frame, the limit baffle and the motor fixing seat are processed by wire cutting. Assembly follows a bottom-up sequence: first the wire-cut chassis, the counterweight blocks and the four-wheel Mecanum drive modules are fixed, then the 3D-printed crank-and-linkage rocking transmission assembly is installed, and finally the 3D-printed lifting seat and the egg-shaped cockpit shell are assembled. During assembly the lengths of the bars and the clearance of the hinges are repeatedly checked, the polyurethane limit stops are adjusted to limit the maximum tilt angle of the cockpit, and a small counterweight is arranged at the bottom to restore the low-centre-of-gravity characteristic of the roly-poly.

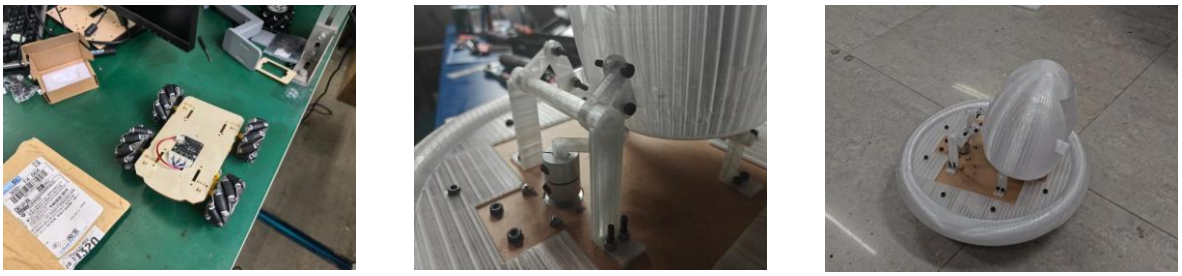


Fig. 9 Assembly and finished prototype
(a) chassis and Mecanum wheels; (b) crank-and-linkage rocking mechanism; (c) finished prototype

Considering that the prototype is used for demonstration only, an industrial PLC was not adopted for the control system; instead, an Arduino main control board was used to build a simple platform (Fig. 10). The hardware includes thin-film pressure sensors, 42 stepper motors with TB6600 drivers, L298N actuators and TT motor drive modules, a micro electric actuator, a sound sensor module and a 24 V regulated power supply. Pressure sensors are arranged under the seat and around the cockpit to collect the occupant weight and the collision impact signals; the rocking mechanism, the seat lifting mechanism and the Mecanum wheel drive are executed by the stepper motors and the TT motors respectively.

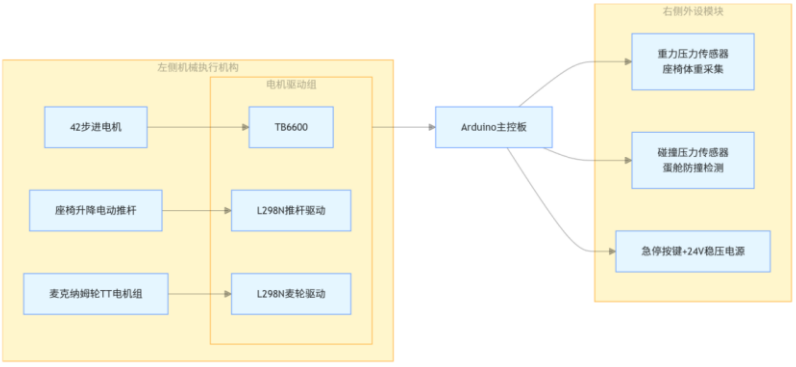


Fig. 10 Block diagram of the control system of the prototype

5.2 Functional Verification

After the mechanical assembly and the electronic control joint commissioning were completed, tests under no-load and simulated conditions were carried out on the prototype, and the verification results are shown in Table 5.

Table 5 Results of the functional verification of the prototype

Item	Test method	Test result
Graded rocking	The collision sensors on the cabin were pressed to simulate light, medium and heavy impacts	The stepper motor drove the crank according to the level, and the cockpit produced small-amplitude low-frequency, medium-amplitude and full-amplitude short-duration swings respectively; the grading logic was correct
Automatic recovery	Driving was stopped after the swing ended; the power was then cut off	The motor reversed to return the crank to the neutral position and the cockpit was restored smoothly; after the power was cut off, it recovered by itself under the gravitational restoring moment of the bottom counterweight
Centre-of-gravity adaptation	Different loads were applied to the seat pressure sensors to simulate occupants of different weights	The program limited the seat lifting stroke according to the load level and stopped automatically when the limit was exceeded
Omnidirectional motion	Commands for straight travel, lateral translation and spinning were input respectively	The four wheels worked together to complete forward and backward travel, lateral translation and on-the-spot 360° spinning
Tilt angle limitation	The driving stroke was continuously increased to the limit	The polyurethane limit stops and the program limit acted together, and the tilt angle was constrained within the design range

The tests show that the prototype can fully reproduce the core functions of the design, that the mechanism moves without jamming and that the bars do not interfere with each other, which verifies the rationality and realizability of the scheme for the whole vehicle. It should be pointed out that the prototype is a scaled-down model, and its mass, inertia and impact load are all reduced in proportion, so the measured tilt angle, recovery time and acceleration cannot be directly equivalent to those of a full-size prototype; subsequent

quantitative tests of the collision acceleration and occupant kinematic response need to be carried out on a 1:1 prototype.

VI. Conclusions

Aiming at the problems of conventional bumper cars, namely a single function, the absence of a bodily sensation of the collision mechanics, and poor occupant adaptability, this paper designed an egg-shaped roly-poly bumper car based on the centre-of-gravity self-balancing principle, and completed the configuration comparison, the mechanism design, the mechanical verification and the prototype verification. The main conclusions are as follows.

(1) A three-layer configuration of "egg-shaped cockpit—crank-and-linkage rocking—counterweighted chassis" is proposed, in which the low-centre-of-gravity counterweight provides a natural restoring moment and electronically controlled rocking achieves controllable swing, forming a dual recovery mechanism of "active regulation + passive fallback" and solving the problems of uncontrollable amplitude and short fatigue life in passive spring rocking.

(2) The configuration comparison shows that under the condition of a collision at 2 m/s with an average impact force of 2700 N, the egg-shaped cockpit has a maximum stress of about 0.29 MPa, a safety factor of about 69 and a fatigue life of more than 100 million cycles, and its space utilization is more than 30% higher than that of the spherical configuration, thus achieving a good balance among strength, space and cost.

(3) The overturning moment of the rocking mechanism at the 20° tilt limit is 51.3 N·m, the required output torque calculated with a safety factor of 2 is 102.6 N·m, and the selected servo gear motor delivers 112.2 N·m, meeting the requirement; the four-bar mechanism satisfies the Grashof criterion and has no dead point; with a 16 mm connecting rod the buckling safety factor is 2.42 and the bending stress is 103.3 MPa, and with a 40 mm × 10 mm rocker arm the bending stress is 76.95 MPa, all of which satisfy the allowable values.

(4) The four-wheel Mecanum chassis achieves omnidirectional motion with a zero turning radius, and the ground contact pressure at a design load of 76.5 kg per wheel is about 0.28 MPa, which is below the allowable interval of the PU roller surface; the gravity-adaptive seat limits the adjustment range of the centre of gravity according to the body weight, taking into account both the safety and the comfort of occupants of different builds.

(5) The prototype verification shows that the functions of graded rocking, automatic recovery, weight-limited seat lifting and omnidirectional motion can all be reproduced, and that the scheme has engineering feasibility.

Future work will proceed in three directions: first, carrying out quantitative tests of the collision acceleration, the occupant kinematic response and the rocking comfort on a 1:1 prototype, so as to improve the safety evaluation index system; second, installing a visual display screen to show in real time the force decomposition of the Mecanum wheels, the motion trajectory of the crank and linkage, and the real-time height of the centre of gravity of the whole vehicle, so as to strengthen the effect of science popularization; and third, optimizing the counterweight and the cockpit structure so as to further reduce the total mass and the manufacturing cost while maintaining the anti-overturning performance.

References

[1] State Administration for Market Regulation, Standardization Administration. GB 8408-2018 Safety specification for large-scale amusement devices[S]. Beijing: Standards Press of China, 2018. (in Chinese)

[2] ZHAO Jiufeng. Simulation study on low-speed collision of bumper cars based on transient dynamics[J]. Process Automation Instrumentation, 2022, 43(4): 26-30. (in Chinese)

[3] SHEN Yong, E Lijun. Comparative study on regulations and standards for amusement devices at home and abroad[J]. China Safety Science Journal, 2010, 20(11): 82-90. (in Chinese)

[4] ZHANG Yong, QIN Pingyan, LIN Weiming, et al. Study on the operating state test system and key technologies for large-scale amusement devices[J]. China Safety Science Journal, 2008, 18(12): 166-171. (in Chinese)

[5] WANG Yinlan, SONG Weike, LIN Weiming. Design risk assessment method for large-scale amusement devices[J]. China Special Equipment Safety, 2014, 30(4): 58-62. (in Chinese)

[6] COHEN A, LEE S, PARK J. Frontal, lateral and free-operation impacts of amusement bumper cars: Vehicle kinematics and occupant kinematics[J]. Safety Science, 2025, 142: 106589.

[7] ASTM International. ASTM F2291-16 Standard practice for design of amusement rides and devices[S]. West Conshohocken: ASTM International, 2016.

[8] ISO. ISO 17842-1:2023 Safety of amusement rides and amusement devices—Part 1: Design and manufacture[S]. Geneva: ISO, 2023.

[9] SMITH J, JOHNSON L. Crashworthiness analysis of foam-filled bumper beams for low-speed impact applications[J]. International Journal of Mechanical Sciences, 2024, 256: 108729.

[10] Standardizing the handling of bumper cars to ensure amusement safety[J]. Quality and Standardization, 2013(4): 27-28. (in Chinese)

[11] ZHAO Jiufeng. Collision response and safety analysis of bumper cars at different speeds[J]. Journal of Luoyang Institute of Science and Technology (Natural Science Edition), 2023, 33(2): 56-60. (in Chinese)